THE IMPACT OF SURFACE CHEMISTRY ON PHOTOELECTROCHEMICAL DEVICE CHARACTERISTICS

Thesis by

Robert Rosenberg

In Partial Fulfillment of the Requirements for the

degree of

Bachelor of Science

Applied Physics

CALIFORNIA INSTITUTE OF TECHNOLOGY

Pasadena, California

June 3, 2011

ABSTRACT

Varying degrees of partial methylation are performed on the (111) surface of p-type Si in order to investigate the role of mixed surface functionality on the device's overall properties. Current-voltage characteristics are acquired in nonaqueous regenerative photoelectrochemical cells with a variety of one-electron redox species. P-type and p/n+ electrodes are evaluated, allowing comparisons between devices where the energy barrier is set by the semiconductor-liquid interface and devices where the energy barrier is set by the buried junction with the heavily doped emitter layer. In contrast to fully methylated or entirely unprotected surfaces, the intermediately methylated devices exhibit mixed monolayers with a disparity in barrier height. Charge transfer across these interfaces is studied, and effects such as pinch-off are considered in the search for a threshold surface composition for acceptable device performance.

INTRODUCTION

Silicon is a well-studied earth abundant semiconductor with a 1.12 eV band gap well suited for solar energy conversion. It has received attention as a candidate photocathode material for artificial photosynthesis applications where incident light excites an electron-hole pair in the semiconductor lattice, and in solution the minority charge carrier is collected to perform electrochemical water splitting. [1] However, exposure to air or water leads to formation of nonstoichiometric native oxide on the silicon surface which strongly degrades device performance. [2] The ability to protect every atop site has been achieved through a two-step chlorination-alkylation procedure which eliminates dangling bonds and can keep devices stable for months, as opposed to the hours of stability exhibited by unprotected hydride terminated silicon surfaces. [3,4] However, incomplete surface functionalization is still likely due to radicals in the ambient atmosphere or the use of microwire device configurations with geometries less conducive to full coverage than the (111) surface. New behaviors arise when there is a mixed monolayer on the surface instead of a single functional group, and we wish to connect the changing conditions for charge transfer at the semiconductor-liquid interface to overall device performance.

Three main parameters from the current-voltage characteristic (Fig. 1) of a semiconductor device give information about its energy conversion properties. The intercept of the current density axis, termed open-circuit voltage (V_{oc}) is the maximum Gibbs free energy that the junction can provide under specific temperature and illumination conditions. [5] The intercept of the potential axis, termed short-circuit current density (J_{sc}) reflects the yield of minority carriers crossing the energy barrier. Each J-V characteristic has a unique maximum power point and fill factor, the final parameter, represents how closely the device approaches the theoretical maximum power output defined by its maximum current and voltage. Fill factor is expressed simply as the ratio $J_{mp}V_{mp}/J_{sc}V_{oc}$. To achieve efficient solar energy conversion, it is necessary to simultaneously optimize the three electrical properties mentioned above. [6]

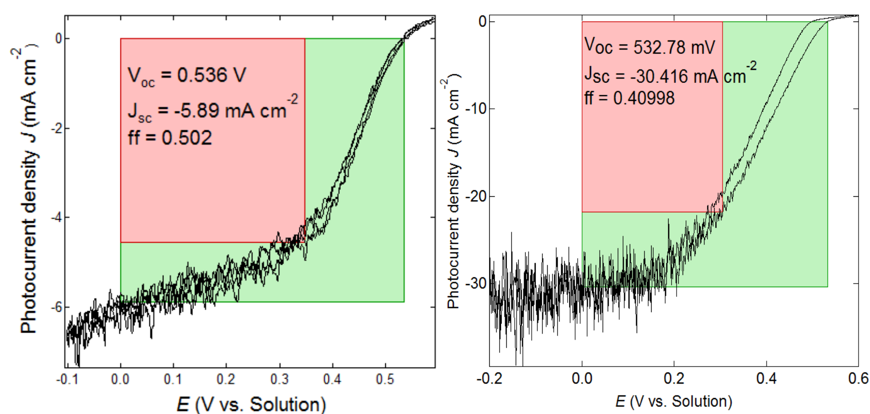

Figure 1: Open-circuit and short-circuit are the corners of the colored area, fill factor is the ratio of red area representing maximum power, to green area representing theoretical maximum power. (a) Current density – voltage characteristic for a p/n+ device tested in $Co(Cp^*)_2^{+/0}$. (b) Data from p-type device tested in $CoCp_2^{+/0}$

In an effort to optimize V_{oc}, it is useful to first consider the theoretical maximum potential. The simplest limit that can be placed on the open-circuit voltage of a semiconductor device is the band gap of the material being used. However, in the absence of extreme light intensity, bulk recombination of the photogenerated electrons and holes will place a stricter restriction on the maximum V_{oc}. [7] There is a dependence on experimental conditions such as temperature, the formal redox potential of the solution, and illumination, and material-specific properties such as minority carrier diffusion length and mobility.[8] All of these parameters are treated as identical for all devices made from the same wafer and tested in the same cell. Therefore, the most important contributing factor is the height of the energy barrier set by the semiconductor-liquid junction or the solid-state junction through which electrons pass before diffusing into solution. Nonidealities in $V_{oc,}$ then, are commonly attributed to a lower than desired barrier height or surface carrier recombination due to deleterious surface states.

The concept of band bending (Fig. 2) is fundamental for understanding and controlling the barrier height of a semiconductor device.[9] The immediate neighborhood of the junction is referred to as the space-charge region because of a local electric field that moves minority carriers across the interface. This local field leads to local changes in electron energies as Fermi levels equilibrate across the junction. The term band bending refers to the shapes of the valence band and conduction band on a band diagram. Before equilibration their energies are constant, but after equilibration their energies vary with distance from the interface. The flat-band region begins a sufficient distance away from the space-charge region, and for the semiconductor-liquid junction the band bending can be expressed as the difference between the flat-band voltage and the solution redox potential. Controlling the charge transfer kinetics at a junction requires control of the band edge positions, and one way to achieve this control is manipulation of the functional group at the device surface. [10]

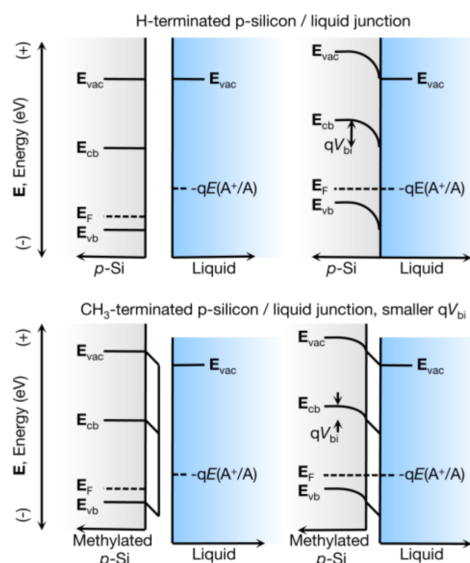

Figure 2: As the Fermi levels of p-Silicon and the redox solution equilibrate, the energy bands at left become spatially dependent, or "bend" as shown at right. Note that surface dipole moments affect barrier height.[11]

The dual need to protect and maintain as large of an energy barrier as possible is the primary motivation to protect electrode surfaces from the formation of deleterious native oxides. [12] This unwanted layer features electrical traps at densities exceeding 10^{11} cm^{-2}, the presence of which facilitates Shockley-Read-Hall recombination of electrons and holes at energies between the valence band and conduction band.[13,14] Another negative effect of native oxide is a strong series resistance, which hinders charge transfer.

At the conclusion of the alkylation procedure, it is assumed that all sites not occupied by the functional group are hydrogen terminated. While hydride terminated silicon behaves extremely well, it unfortunately degrades within under an hour of exposure to ambient air. The methyl ligand is preferred due to its ability to cover every atop site on the silicon surface.[3] Due to its small size, steric clashing does not take place as it does with many other functional groups. However, a wide range of different effects can be achieved by varying surface functionality. For example, the methyl ligand has a dipole moment of 0.38 eV which is a significant shift to the total barrier height.[15] Short chain alkyls resist charge transfer across the interface more as chain length increases, up to the 6th carbon but not afterward.[3] Experiments have also been performed using perflurophenylated surfaces, whose dipole is in the opposite direction. When varying surface functional group it is also important to consider the cross section of the molecule, which determines surface coverage and in turn sets a minimum level of vulnerability to native oxide growth.

While hydride termination is not stable, it is important to note that H-term surfaces perform extremely well. The trap state densities are below 10^{-8} cm^{-2} and in solutions with mid-gap formal potentials, maximum open-circuit voltage is significantly higher for hydride than for methyl. Related studies (Fig. 3) performed in the Lewis group demonstrate a shift in photovoltage caused by surface dipole effects, but also demonstrate that for sufficiently negative solutions carrier inversion is reached, which has a much stronger influence and causes the separate trends to converge at the same maximum V_{oc} value. A potentially beneficial mix of surface coverage could combine the higher V_{oc} from the H-terminated devices and the stability of the CH_3-terminated devices.

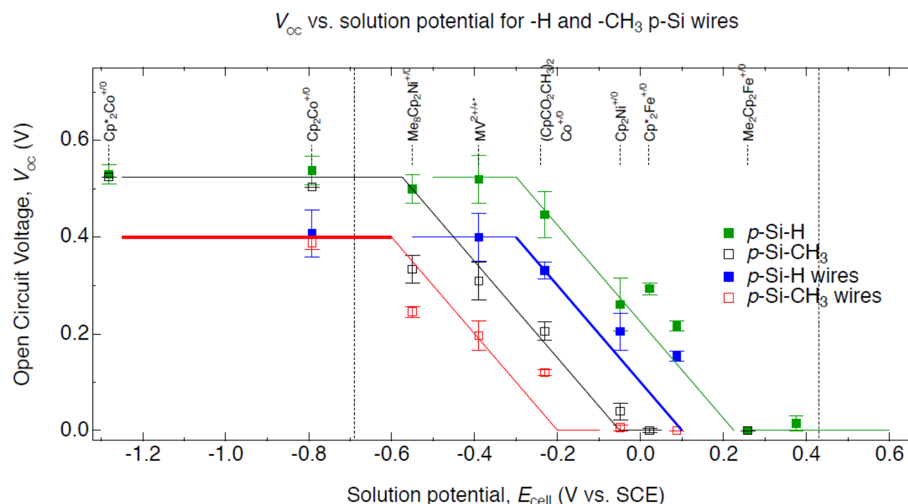

Figure 3: Dependence of open-circuit voltage on surface functionality, redox couple, and device configuration.[11]

Devices are tested in contact with a variety of one-electron redox species. The potentials range from cobaltocene/cobaltocenium which is so negative (-0.8 V vs. SCE) that V_{oc} of p-type devices is limited by carrier inversion, to ferrocene/ferrocenium which is sufficiently positive (+0.25 V vs. SCE) that the carrier inversion limit for n-type open-circuit voltage is achieved. Intermediate voltages are often achieved by adjusting the composition of the organic rings with the substitution of methyl groups or the addition of methyl esters. At intermediate voltages, devices give a lower voltage limited by Fermi level pinning, but these solutions offer the advantage of being able to simultaneously test p-type and n-type devices. More specifically, if the redox couple exhibits a low barrier height, V_{oc} will scale linearly with $E(A^+/A)$, but the trend does not continue for more extreme potentials because the open-circuit voltage reaches the limit set by carrier inversion. [16] The term inversion refers to the applied bias voltage making the minority carrier more abundant at the semiconductor-liquid interface than the majority carrier.

Partially methylated surfaces are expected to feature nanometer scale domains of oxide and methyl, with a higher barrier height in the methylated regions.[17] The size of the oxide regions is important due to the pinch-off effect, first discovered with metal-semiconductor contacts.[18] For surfaces with mixed domains of high and low barrier heights, the low barrier height regions must exceed a minimum size, on the order of the depletion width of the semiconductor, or their effective barrier height will increase to the point where current is forced to pass through the high barrier regions.[19] If the oxide regions that form are smaller than this critical size then the high barrier of the methylated regions will screen or “pinch off” the low barrier native oxide domains. This critical radius is also governed by the difference in barrier heights, dopant concentrations, temperature, and both built-in and applied voltages.[15] The pinch off effect has significant implications on the level of oxidation that a successful device can tolerate. For example, if methylation proceeds to an extent that the only remaining spaces to oxidize are smaller than the critical pinch-off size, then further methylation could be

unnecessary. The importance of the pinch-off effect cannot be overlooked; it is speculated that it allows up to 10% coverage of a low barrier height material that would have significant harmful effect with only 1% coverage otherwise.[18]

We assume that both the surface functionalization reaction and the oxidation reaction take place according to Langmuir adsorption theory.[20] According to this model, adsorption rates vary with the number of available sites, adsorbed molecules do not interact with each other, and adsorbed molecules do not move. As sites get filled the adsorption rate slows, causing surface coverage to vary linearly with the inverse of time or concentration. This is the basis for establishing a conversion between the measured experimental parameter methylation time and fractional methyl coverage, which should govern device behavior. To determine the coefficients of this linear relation, a fit is performed on X-ray photoelectron spectroscopy data. We assert that the fractional methyl coverage on the Si (111) surface, Θ, varies with time according to the Langmuir equation:

$$\theta = \frac{\alpha t}{1+\alpha t}$$

EXPERIMENTAL METHODS

For all experiments, B doped p-Silicon wafers were used with resistivity ~ 0.25 Ω cm. The first step in creating p/n+ buried junctions is to grow a thermal oxide layer by flowing O_2 at 2 liters/min at 1100°C for 90 minutes. Next, S1813 photoresist is applied to the back side using a spin-coater at 3000 rpm for 1 minute, followed by a 2 minute soft bake at 120°C. To expose the front side, samples are etched with Buffered HF Improved for 2 minutes, and after rinsing, acetone is applied to the back to remove the photoresist. Samples were loaded onto a quartz boat between solid source CeP_5O_{14} diffusion wafers (Saint-Gobain, PH-900 PDS) and heated at 850 °C for 10 min under a N_2 ambient in a tube furnace[21]. The junction properties are tested using a mercury contact probe.

A two-step procedure (Fig. 4) was used to functionalize all surfaces, complete halogenation followed by different levels of partial methylation.[4] First, a very reactive Cl-terminated surface is prepared by exposing samples to a saturated solution of PCl_5 in chlorobenzene with a benzoyl peroxide initiator, maintained at 90°C for 45 minutes. After thorough rinsing, the surface is exposed to a 1M solution of alkyl Grignard (CH_3MgCl) in tetrahydrofuran at 60-70°C. Times are varied to create mixed surfaces of different compositions, but a few hours are sufficient to achieve full coverage. Both reactions are carried out in an inert N_2 atmosphere, and both p-type and p/n+ samples are quickly HF etched immediately prior to the alkylation reaction to remove any recently grown native oxide. Following surface functionalization, samples are stored in methanol, sonicated in methanol, sonicated in isopropanol, and dried thoroughly under a stream of argon.

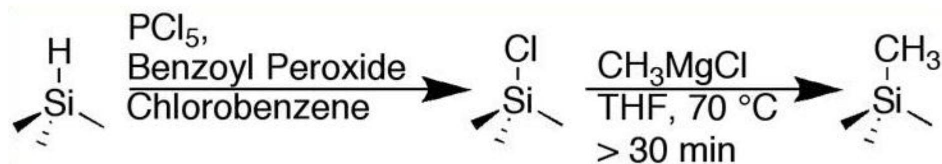

Figure 4: Lewis Group two-step methylation process

Once the silicon is methylated, it has to be assembled into an electrode for testing in a photoelectrochemical cell. Samples are first cut using a scribe into smaller chips with areas of roughly 0.5 cm^2. The unpolished back side is scratched to facilitate the application of a gallium-indium eutectic which allows a tinned copper wire to make a back contact to the silicon. The back is covered with silver paint, and epoxy is used to seal the assembly into a 6mm diameter glass tube.

The configuration (Fig. 5) used for device testing depends on the redox couple, and more specifically on whether or not stable forms exist for both the oxidized and reduced species. Both configurations employ a Pt wire reference and a Pt mesh counter electrode. Stirring is maintained, but it is still desirable to position the reference electrode as close as possible to the working electrode to avoid errors arising from nonuniform solution potential. The counter

electrode, which acts as a source of free electrons when the cell is operated under cathodic conditions, is positioned farther away from the silicon device. All redox couples are dissolved in acetonitrile along with 1M lithium perchlorate as a supporting electrolyte. An ELH light source is calibrated using a photodiode to provide 1 sun of Air Mass 1.5 illumination which is normal to the silicon surface.

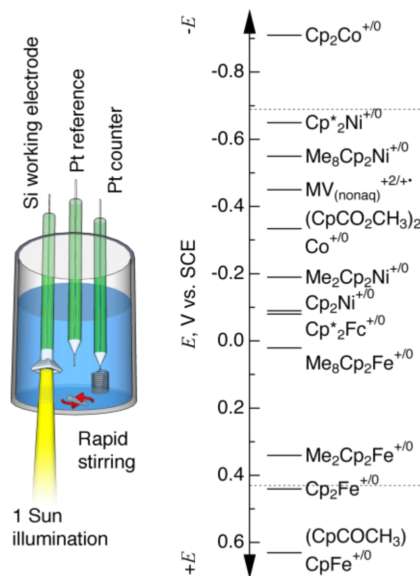

Figure 5: At left, a schematic of a three electrode photoelectrochemical cell configuration. The working electrode is illuminated from below, rapid stirring is maintained, and a Pt wire reference and Pt mesh counter are used. At right, a list of redox potentials relative to SCE.

XPS data were collected using a Surface Science Instruments M-Probe system controlled by ESCA25 Capture (Service Physics, Bend OR; V5.01.04) software. The monochromatic x-ray source was the 1486.6 eV Al Kα line, directed at 35° to the sample surface. Emitted photoelectrons were collected by a hemispherical analyzer that was mounted at an angle of 35° with respect to the sample surface. Low-resolution survey spectra were acquired between binding energies of 1-1100 eV. Higher-resolution detailed scans, with a resolution of ~0.8 eV, were collected on individual XPS lines of interest .The sample chamber was maintained at $< 5 \times 10^{-9}$ Torr. The XPS data were analyzed using the ESCA25 Analysis Application (V5.01.04). The Si $2p_{1/2}$ peak was constrained to be equally wide, half as high, and shifted by +0.67 eV relative to the Si $2p_{3/2}$ peak.[4] Oxide coverage was primarily determined by comparing the sum of Si $2p_{1/2}$ and Si $2p_{3/2}$ peak areas to the area of the oxygen-shifted peak. The O 1s peak was also measured to verify the silicon result, and the two correlated nicely. C 1s peaks were measured as well, but adventitious species interfered with the ability to discern methyl peaks.

If both the oxidized and reduced forms of the redox couple exist in a stable form, it is straightforward to prepare a solution where the concentrations of both species are high enough to prevent either from getting depleted at the silicon surface. It is also straightforward to prepare the solution with the two forms in the proper ratio, which will remain constant when the

reversible cyclic voltammetry reactions are performed. However, if only one stable form exists, the other must be generated in situ using additional electrodes. An additional counter electrode, a Pt mesh separated from the solution by a frit, passes electrons to produce the second species. Additionally, a $Ag^{+/0}$ reference electrode is prepared by filling a fritted glass tube with the identical mixture of acetonitrile and lithium perchlorate as the photoelectrochemical cell, adding 10-100 mM of silver nitrate, and immersing a silver wire. This secondary reference electrode allows a precise and standard definition of solution potential. First, the formal potential is measured as the difference between the anodic and cathodic peaks of a cyclic voltammagram. After the second species has been generated, another cyclic voltammagram is acquired, and the shift in potential, following the Nernst equation, indicates the ratio of the two forms of the redox couple. It is common to repeatedly adjust concentrations if several devices are being tested in the same cell.

RESULTS

A. X-Ray Photoelectron Spectroscopy

The Si 2p XPS peak (Fig. 6) near 99 eV gives a reliable indication of how much the surface has oxidized. The relevant parameters are the relative areas of the bulk Si 2p and the oxygen shifted peak near 102.5 eV. Additionally, the O 1s peak area was compared to the Si 2p in order to verify any observed trends.

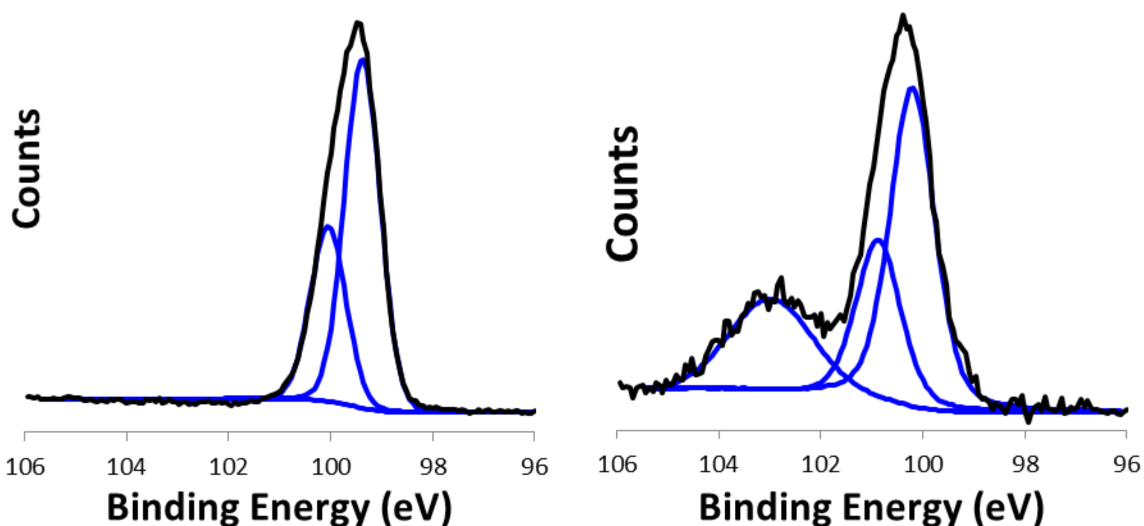

Figure 6: (a) P-type Si 2p peak at 99 eV with no visible oxidation (b) p/n+ Si 2p region with an additional peak at 103 eV attributed to oxidized silicon.

i. P-type

Following methylation, these samples (Fig. 7) spent less than 3 hours exposed to ambient atmosphere. For this reason, only 4 of the 10 samples showed any silicon oxide signal whatsoever. This makes the trends in O:Si ratio especially valuable, because each sample provided a usable signal.

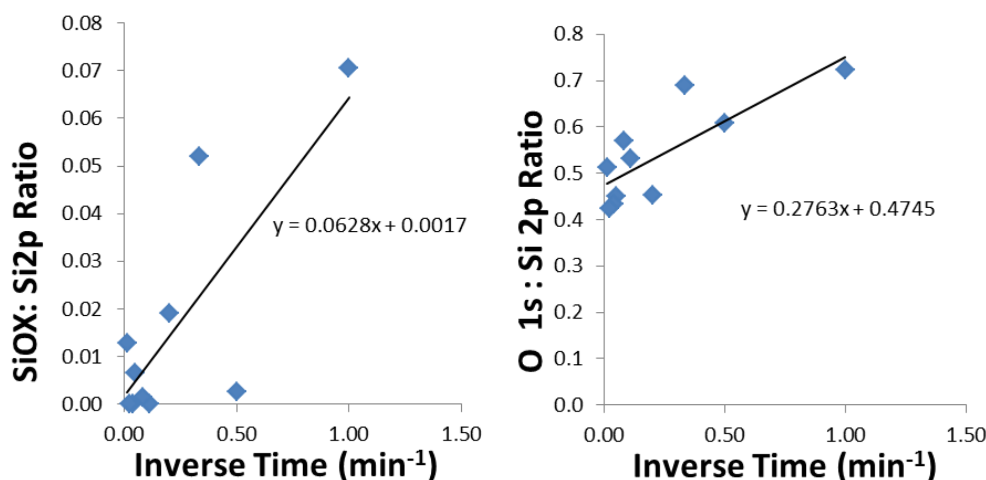

Figure 7: Langmuir adsorption theory predicts a linear relationship between inverse methylation time and oxide coverage. (a) Oxide coverage represented by SiOx:Si2p, but several samples exhibited no oxide signal. (b) Oxide coverage represented by O 1s: Si 2p

ii. Buried p/n+ solid state junction

Spectra for these samples (Fig. 8) were acquired two months after methylation was performed. Despite being stored in an inert Ar atmosphere for much of this time, they still exhibited oxygen signals roughly 20 times stronger than the p-type samples which had less exposure to ambient conditions. There is a much stronger correlation in trends given by oxygen and silicon spectra, and these trends are in general agreement with Langmuir theory. The roughly 20-fold difference in oxide coverage resulting from difference in elapsed time between surface functionalization and acquisition of spectra should serve as a powerful reminder that 100% methylation should be expected to persist over large time scales.

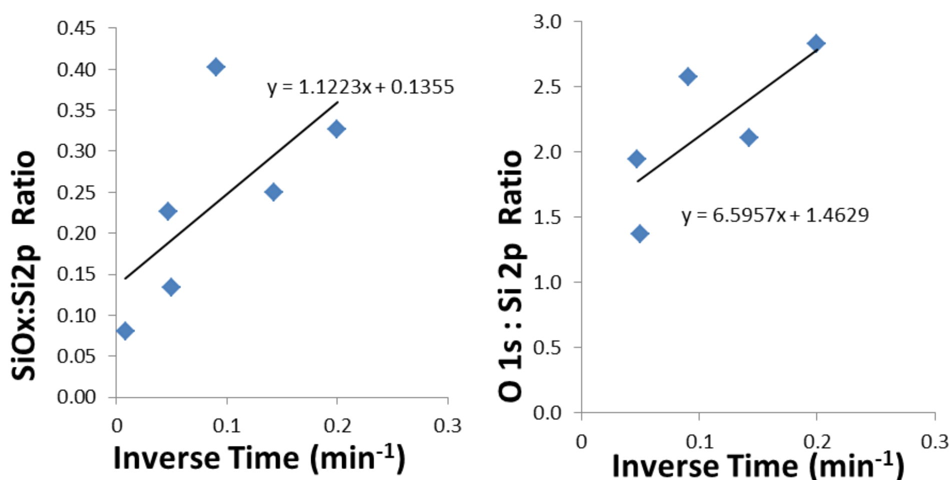

Figure 4: Relation between (a) oxide area and (b) oxygen area to unshifted silicon peak area. The trends are effectively identical Note that (a) is used to provide the conversion from methylation time to assigned surface coverage.

iii. Conversion from methylation time to assigned surface coverage

Details for the derivation of the relationship between reaction time and surface coverage are provided in the appendix.

$$\theta(t) = \frac{1.2223\,(t-180*0.05)+0.1355*180*t(1-0.05)}{(1.2223+0.1355*180)t} = \frac{24.393t-11.001}{25.6123t}$$

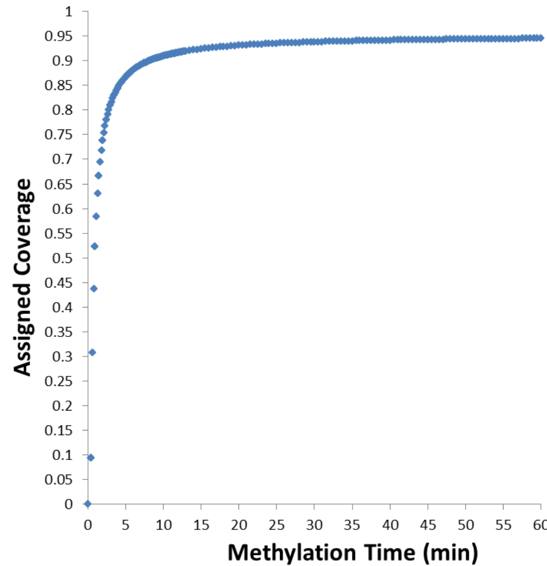

Figure 9: Conversion between methylation time and assigned methyl surface coverage. Parameters taken from p/n+ XPS spectra

B. P-type devices in Methyl Viologen

A batch of p-type devices from the same wafer was tested in methyl viologen (Fig. 9) along with preexisting H-terminated and fully CH_3-terminated devices. It was found that for the intermediately methylated devices, V_{oc} improved at a slow, steady rate with increasing methylation time. However, the samples which were barely methylated exhibited the highest voltages. This is somewhat unexpected, but is also somewhat consistent with the improved voltage that H-terminated devices exhibit compared to their CH_3 terminated counterparts. Fill factor data exhibits the expected trend of improved performance with increased methylation more strongly, at least for the set of devices made from the same starting wafer.

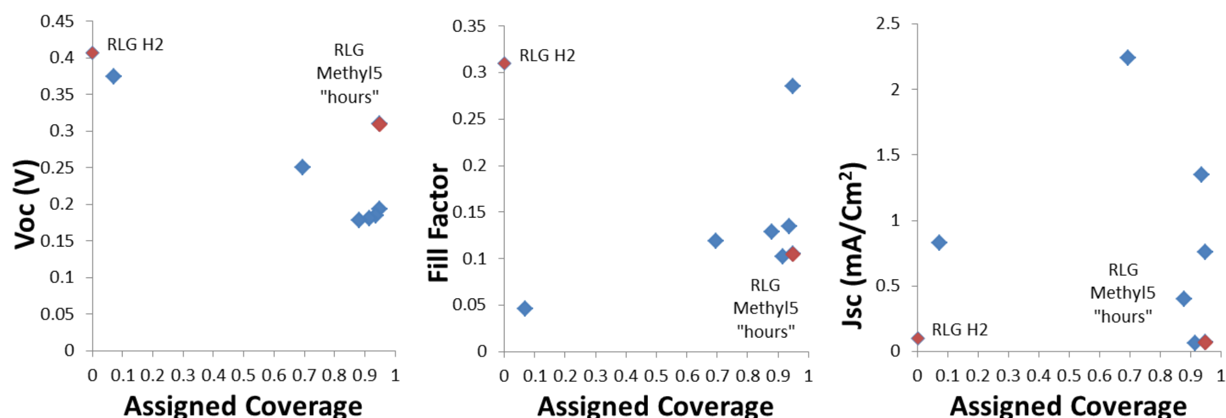

Figure 9: (a) Open circuit voltage vs. assigned coverage of methyl groups on the p-Si electrode surface in contact with $MV^{2+/+}$ (b) Fill factor of the same devices showing roughly the same trend (c) Short circuit current densities were low and showed no clear relationship to methylation time

C. P-type devices in cobaltocene

A batch of p-type devices from the same wafer was tested simultaneously in cobaltocene (Fig. 10). Because no photodiode was available, light intensity was judged to be effectively 1 sun when a freshly HF treated H-terminated electrode yielded a current density >25mA/cm^2. These devices performed the best of all devices tested.

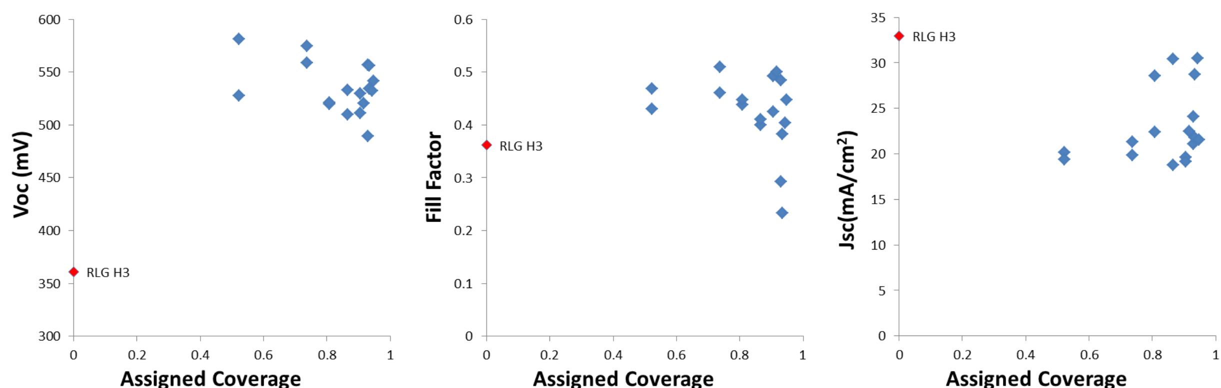

Figure 10: P-type devices in $CoCp_2^{+/0}$ yielded the highest (a) open-circuit voltages, (b) fill factors, and (c) short-circuit current densities.

D. p/n+ devices in decamethyl cobaltocene

A set of p/n+ devices (Fig. 11) was doped, prepared, and tested simultaneously in decamethyl cobaltocene. The trends in open circuit voltage contradict the theory which predicts that buried junction devices should have a V_{oc} set exclusively by the dopant concentrations in the buried junction and the temperature.[22] While it is plausible that a secondary barrier at the surface could impact voltage, the theory asserts that since the n+ layer is effectively metallic, making the depletion width so small that we expect tunneling across any barrier.

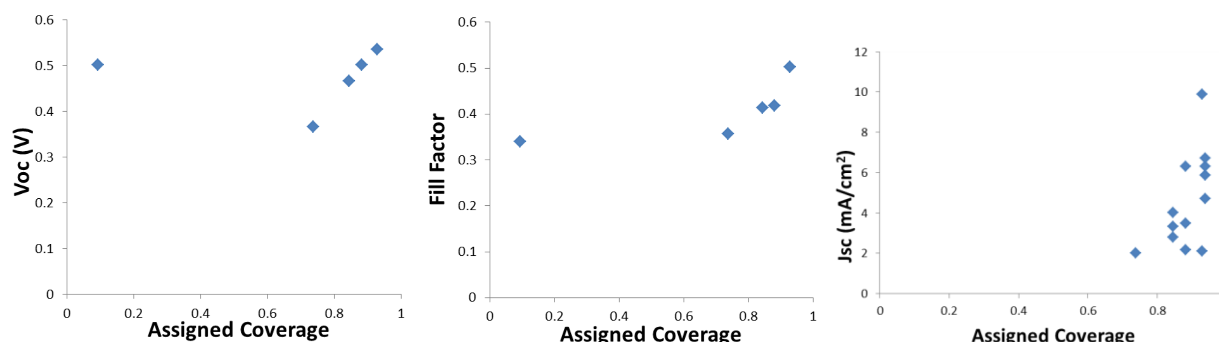

Figure 11: (a) Open circuit voltage data for p/n+ devices in Co(Cp*)$_2$. (b) Fill factor of the same selected devices. (c) Short-circuit current density shows a less clear relationship to assigned surface coverage.

E. p/n+ devices in 1-1' dicarbomethoxy cobaltocene

A set of p/n+ devices was tested (Fig. 12) in 1-1' dicarbomethoxy cobaltocene, synthesized by D. Knapp of the Lewis Group according to literature methods.[23] While there were too many of these devices to dope all of them at once, the diode characteristics were verified through Hg contact measurements (Fig. 13) and all fit exponential behavior at forward bias very well. Both sets of devices show fill factor increasing steadily with Grignard time, as expected. The shift in voltages between Co(Cp*)$_2$ for the first set and 1-1' dicarbomethoxy cobaltocene is consistent with the theory for limiting Voc values.

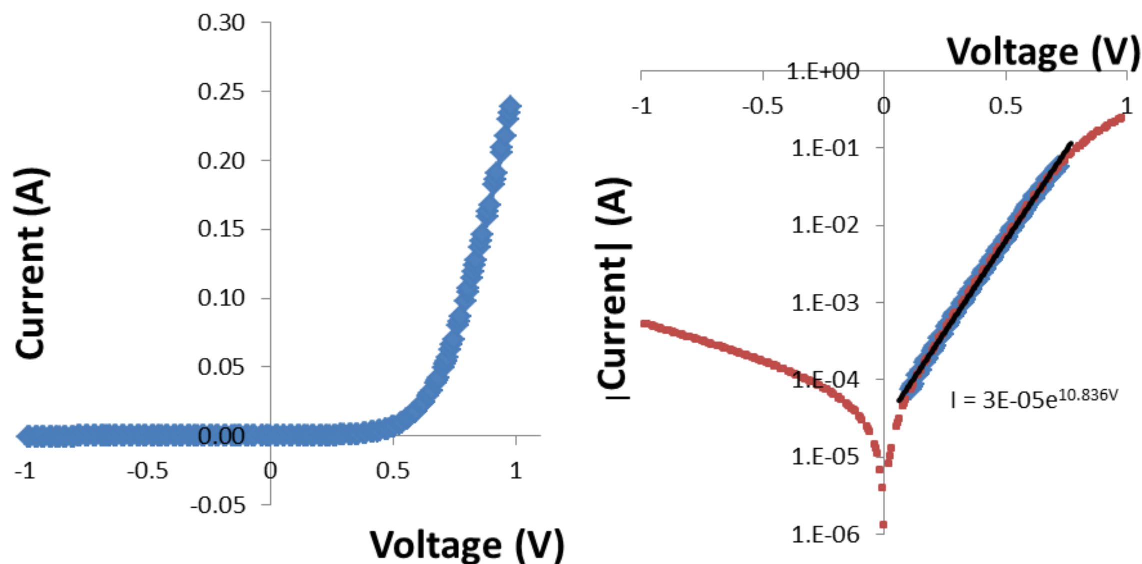

Figure 12: Representative Hg contact probe data to verify the diode properties of p/n+ buried junctions. (a) All data (b) Forward bias, fit to an exponential function.

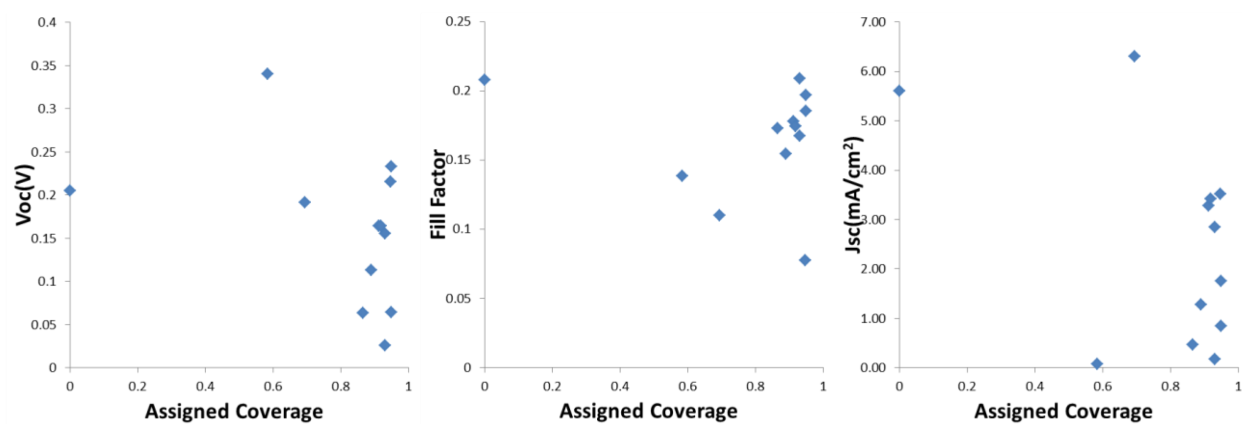

Figure 13: (a) Open-circuit voltage data for p/n+ devices in 1-1' dicarbomethoxy cobaltocene. (b) Fill factor of same devices. (c) Short-circuit current density is poorly related to the extent of methylation. P-type devices tested at the same time are labeled explicitly.

DISCUSSION

Across all sets of devices, trends in open-circuit voltage were the most significant. Using redox couples with mid-gap formal potentials allowed the observation of a reduced V_{oc} due to surface dipole effects which does not occur for the more negative redox solutions where the condition of carrier inversion is achieved. The use of these less negative redox species could also partially explain most devices' current densities being significantly lower than the 25-30 mA/cm^2 that good devices are supposed to yield. The fact that trends were still observed for $CoCp_2^{+/0}$ and $Co(Cp*)_2^{+/0}$ indicates that other factors in addition to the dipole moment impact the charge transfer at the semiconductor-liquid interface. The most significant of these is pinch-off, where high barrier regions screen regions of lower barrier height on a mixed surface. The strongest evidence for this is that for high values of surface coverage, device performance improves as surfaces are increasingly methylated. Additionally, devices with low values of surface coverage exhibited superior performance. This is due to an advantageous combination of the pinch-off effect and the surface dipole field effects. While the original pinch-off experiment was focused on entirely removing the influence of low barrier height regions by covering a large proportion of the surface area with high barriers, we consider a surface at mainly low barrier height with small high barrier domains. Due to pinch-off, a disproportionately large amount of the photogenerated carriers can pass across high barriers which only cover a small portion of the surface, which is beneficial. However, the detrimental effects of the surface dipole are greatly reduced when the methyl only exists in small patches and covers a very small amount of the electrode surface.

CONCLUSION

The initial expectation was that using methylation to protect the silicon surfaces from deleterious native oxide would improve device performance. If this is judged based on fill factor, the expectation generally holds though many points do not fall in line, perhaps due to inconsistencies in electrode fabrication and imperfect environmental control. The data for open circuit voltage is more puzzling, because for all sets of devices, the samples which spent the least amount of time in the Grignard outperformed their counterparts who spent intermediate amounts of time reacting. This is expected for the p-type devices that should be sensitive to fields between the semiconductor and solution, but not for the buried junctions.

These experiments show that surface functionality plays an important role in the performance of a photoelectrochemical device, which is to be expected given that all photogenerated charges in the semiconductor must pass through this layer before it can do work in solution. Preventing oxidation is desirable, but more work should be done to investigate the behaviors of devices that are only slightly methylated and have exhibited better performance than expected.

It would be instructive to repeat these experiments with microwire devices, because due to the increased surface area they should be more vulnerable to the effects of surface chemistry.[24] Methylation has already been shown to stabilize nanowires and it would be interesting to trace this through the intermediate states.[25]

Additional future work could measure trends in surface recombination velocity with varied surface coverage, because it is one of the most sensitive parameters to the effects of native oxide. Additionally, scanning tunneling microscope imagery of the silicon surfaces would allow a much more conclusive determination of the relative sizes of the oxide and methyl domains than prediction from theory can provide.

APPENDIX

Derivation for the conversion between methylation time and assigned surface coverage

According to the Langmuir equation, Θ will never reach a value of 1 in finite time. For this reason, we define a time T_m after which the surface coverage will reach a "maximum" value of 1-δ.

$$\theta = \frac{\alpha t}{1+\alpha t}$$

Fitting XPS peak area ratios provides us with data of the form

$$A(SiO_x):A(Si\ 2p) = \frac{x}{t} + y$$

The XPS peak ratios are proportional to oxide coverage. Assuming each site is either methylated or oxidized:

$$\theta_{oxide} = 1 - \theta = C\left(\frac{x}{t} + y\right)$$

The constant C is a function of x,y,δ, and T_m:

$$1 - \theta(T_m) = \delta = C\left(\frac{x}{T_m} + y\right)$$

$$C = \frac{\delta}{\frac{x}{T_m}+y}$$

This relation allows us to solve for Θ(t,x,y,T_m,δ):

$$\frac{x}{t} + y = \frac{1-\theta}{C} = \left[1 - \frac{\alpha t}{1+\alpha t}\right] * \frac{\frac{x}{T_m}+y}{\delta} = \frac{\frac{x}{T_m}+y}{\delta}\frac{1}{1+\alpha t}$$

$$\delta(1+\alpha t)\left(\frac{x}{t} + y\right) = \frac{x}{T_m} + y$$

$$\alpha t = \frac{\frac{x}{T_m}+y}{\delta\left(\frac{x}{t}+y\right)} - 1 = \frac{\left(\frac{x}{T_m}+y\right)t}{\delta(x+ty)} - 1 = \frac{(x+yT_m)t}{\delta T_m(x+ty)} - 1 = \frac{(x+yT_m)t - \delta T_m(x+ty)}{\delta T_m(x+ty)} = \frac{x(t-\delta T_m)+yT_m t(1-\delta)}{\delta T_m(x+ty)}$$

$$\theta = \frac{\alpha t}{1+\alpha t} = \frac{\frac{x(t-\delta T_m)+yT_m t(1-\delta)}{\delta T_m(x+ty)}}{\frac{(x+yT_m)t}{\delta T_m(x+ty)}} = \frac{x(t-\delta T_m)+yT_m t(1-\delta)}{(x+yT_m)t}$$

Using x = 1.2223, y = 0.1355, T_m = 180 minutes, δ = 0.05 we obtain assigned surface coverage:

$$\theta(t) = \frac{1.2223\,(t-180*0.05)+0.1355*180*t(1-0.05)}{(1.2223+0.1355*180)t} = \frac{24.393t-11.001}{25.6123t}$$

ACKNOWLEDGEMENTS

Many thanks to Nate Lewis for making this extremely rewarding experience possible, toRon Grimm for teaching me nearly everything I know, to Shane Ardo for helping me get on the right track when I needed it most, to Oskar Painter and Sandra Troian for their valuable advice, an d to CX Xiang, Mike Walter, Matt Bierman, Nick Strandwitz, Leslie O' Leary, Liz Santori, Jacob Good,Dan Turner-Evans, Andrew Meng, Jessie Ku, and the Lewis group as a whole for being so friendly and knowledgeable.

BIBLIOGRAPHY

(1) Khaselev, O.; Bansal, A.; Turner, J. A. *International Journal of Hydrogen Energy* **2001**, *26*, 127.
(2) Morita, M.; Ohmi, T.; Hasegawa, E.; Kawakami, M.; Ohwada, M. *Journal of Applied Physics* **1990**, *68*, 1272.
(3) Bansal, A.; Lewis, N. S. *The Journal of Physical Chemistry B* **1998**, *102*, 4058.
(4) O'Leary, L. E.; Johansson, E.; Brunschwig, B. S.; Lewis, N. S. *The Journal of Physical Chemistry B* **2010**, *114*, 14298.
(5) Lewis, N. S. *Journal of The Electrochemical Society* **1984**, *131*, 2496.
(6) Lewis, N. S. *Accounts of Chemical Research* **1990**, *23*, 176.
(7) Rosenbluth, M. L.; Lieber, C. M.; Lewis, N. S. *Applied Physics Letters* **1984**, *45*, 423.
(8) Rosenbluth, M. L.; Lewis, N. S. *The Journal of Physical Chemistry* **1989**, *93*, 3735.
(9) Bard, A. J.; Bocarsly, A. B.; Fan, F. R. F.; Walton, E. G.; Wrighton, M. S. *Journal of the American Chemical Society* **1980**, *102*, 3671.
(10) Hilal, H. S.; Turner, J. A. *Electrochimica Acta* **2006**, *51*, 6487.
(11) Grimm, R. L.; Bierman, M. J.; O'Leary, L. E.; Lewis, N. S. In preparation.
(12) Ferry, L. L. *Electrochimica Acta* **1990**, *35*, 413.
(13) Shockley, W.; Read, W. T. *Physical Review* **1952**, *87*, 835.
(14) Royea, W. J.; Juang, A.; Lewis, N. S. *Applied Physics Letters* **2000**, *77*, 1988.
(15) Maldonado, S.; Plass, K. E.; Knapp, D.; Lewis, N. S. *The Journal of Physical Chemistry C* **2007**, *111*, 17690.
(16) Laibinis, P. E.; Stanton, C. E.; Lewis, N. S. *The Journal of Physical Chemistry* **1994**, *98*, 8765.
(17) Stranick, S. J.; Parikh, A. N.; Tao, Y. T.; Allara, D. L.; Weiss, P. S. *The Journal of Physical Chemistry* **1994**, *98*, 7636.
(18) Rossi, R. C.; Lewis, N. S. *The Journal of Physical Chemistry B* **2001**, *105*, 12303.
(19) Freeouf, J. L.; Jackson, T. N.; Laux, S. E.; Woodall, J. M. *Journal of Vacuum Science and Technology* **1982**, *21*, 570.
(20) Langmuir, I. *Journal of the American Chemical Society* **1916**, *38*, 2221.
(21) Warren, E. L.; Boettcher, S. W.; Walter, M. G.; Atwater, H. A.; Lewis, N. S. *The Journal of Physical Chemistry C* **2010**, *115*, 594.
(22) Sze, S. M.; Ng, K. K. *Physics of semiconductor devices*; Wiley-Interscience, 2007.
(23) Rosenblum, M.; North, B.; Wells, D.; Giering, W. P. *Journal of the American Chemical Society* **1972**, *94*, 1239.
(24) Kayes, B. M.; Atwater, H. A.; Lewis, N. S. *Journal of Applied Physics* **2005**, *97*, 114302.
(25) Haick, H.; Hurley, P. T.; Hochbaum, A. I.; Yang, P.; Lewis, N. S. *Journal of the American Chemical Society* **2006**, *128*, 8990.